 CMES, vol.16, no.2, pp.103-114, 2006

Investigations on the Accuracy and Condition Number for the Method of Fundamental Solutions

C.C. Tsai[1], Y.C. Lin[2], D.L. Young[2,3] and S.N. Atluri[4]

Abstract: In the applications of the method of fundamental solutions, locations of sources are treated either as variables or *a priori* known constants. In which, the former results in a nonlinear optimization problem and the other has to face the problem of locating sources. Theoretically, farther sources results in worse conditioning and better accuracy. In this paper, a practical procedure is provided to locate the sources for various time-independent operators, including Laplacian, Helmholtz operator, modified Helmholtz operator, and biharmonic operator. Wherein, the procedure is developed through systematic numerical experiments for relations among the accuracy, condition number, and source positions in different shapes of computational domains. In these numerical experiments, it is found that in general very good accuracy is achieved when the condition number approaches the limit of equation solver, which is a number dependent on the solution scheme and the precision. The proposed procedure is verified for both Dirichlet and Neumann boundary conditions. The general characteristics in these numerical experiments demonstrate the capability of the proposed procedure for locating sources of the method of fundamental solutions for problems without exact solutions.

keyword: Method of fundamental solutions, Condition number, Location of sources, Laplacian, Helmholtz operator, Modified Helmholtz operator, Biharmonic operator

1 Introduction

In the recent years, the meshless or mesh-free methods have received a considerable attention as alternative numerical schemes to the classical mesh-dependent numerical methods, such as the finite difference method (FDM), the finite element method (FEM), the finite volume method (FVM), and the boundary element method (BEM). Roughly speaking, the meshless or mesh-free methods can be divided into two categories. The first one is domain-type methods in which both the differential equations and boundary conditions are approximated, such as the Kansa's method (or multiquadrics (MQ) method) [Kansa (1990A, 1990B), Li, Cheng and Chen (2003), Young, Jane, Lin, Chiu and Chen (2004), Young, Chen and Wong (2005)] as well as the meshless local Petrov-Galerkin method (MLPG) [Wordelman, Aluru and Ravaioli (2000), Lin and Atluri (2000), Kim and Atluri (2000), Atluri (2004), Han and Atluri (2004)]. The second one is boundary-type methods where only boundary conditions are collocated, such as the method of fundamental solutions (MFS) [Kupradze and Aleksidze (1964), Mathon and Johnston (1977), Lyngby (1981), Bogomolny (1985), Smyrlis and Karageorghis (2001), Tsai, Young and Cheng (2002), Smyrlis and Karageorghis (2004), Chen, Fan, Young, Murugesan and Tsai (2005), Hon and Wei (2005), Young and Ruan (2005), Young, Tsai, Lin and Chen (2006)] and the MLPG [Atluri (2004)]. In this paper, we only concentrate on how to locate the sources of the MFS.

The MFS is first proposed by Kupradze and Aleksidze (1964). Originally, the sources of MFS are considered as unknown variables and solved by nonlinear optimization [Mathon and Johnston (1977)]. Later, Bogomolny (1985) improved the theoretical fundamentals of the MFS in considering *a priori* known positions of sources. As a result, the MFS becomes easier and more efficient in practical implementations. However, the ill-conditioning and the locations of source points are numerically problematic. Smyrlis and Karageorghis (2001) have researched the issue for the standard MFS, with the same number of source and collocation points, for harmonic problems in a disk. They suggested rotation and normalization to

[1] Department of Information Technology, Toko University, Chia-Yi County, 61363, Taiwan
[2] Department of Civil Engineering and Hydrotech Research Institute, National Taiwan University, Taipei, 10617, Taiwan
[3] Corresponding author, Email: dlyoung@ntu.edu.tw
[4] Center for Aerospace Research and Education, University of California, Irvine, 5251 California Ave, Suite 140, Irvine, CA 92612, USA

overcome the problems of ill-conditioning and provided mathematical analysis for the issues. Later, Smyrlis and Karageorghis (2004) revisited the same issue by using the least-square MFS, which has more collocation points than source points.

In this paper, we provide a practical procedure to locate the sources in the MFS, which is based on general relations among the error, source locations, and condition number. Theoretically, it is proved that worse conditioning [Lyngby (1981)] and better accuracy [Mathon and Johnston (1977), Bogomolny (1985)] are resulted when the sources are located farther. In our numerical experiments, it is found that best accuracy can be obtained when the condition number approaches the limit of the equation solver, which is a number dependent on the precision and solution scheme. The following computational domains are considered: a circle, a square, a rectangle, and a peanut. Moreover, the following operators are included: the Laplacian, Helmholtz operator, modified Helmholtz operator and biharmonic operator. The MFS formulations, condition number and error, boundary collocation points and source points, theoretical statements, numerical results and discussions, as well as conclusions are provided in the following sections.

2 MFS formulations

We consider the boundary value problem

$$\begin{cases} Lu = 0 \ in \ \Omega \\ Bu = f \ on \ \Gamma \end{cases} \tag{1}$$

where u is the dependent variable to be solved, Ω is the considered computational domain, Γ is the boundary of Ω, L is the partial differential operator of the problem, and B is the differential operator associated with the augmented function f of the boundary condition.

In the MFS, the solution u is approximated by

$$u_N(\mathbf{x};\mathbf{s},\mathbf{c}) = \sum_{i=1}^{N} c_i G(\mathbf{x};\mathbf{s}_i) \tag{2}$$

where N is the number of source points, $\mathbf{c} = (c_1, c_2, ..., c_N)$ are the undetermined source intensities, $\mathbf{s} = (\mathbf{s}_1, \mathbf{s}_2, ..., \mathbf{s}_N)$ are the positions of the *a priori* known sources whose locations are the major considerations of the present paper, and $G(\mathbf{x};\mathbf{s})$ is the fundamental solution defined by

$$-LG(\mathbf{x};\mathbf{s}) = \delta(\mathbf{x}-\mathbf{s}) \tag{3}$$

for the operators considered in this paper, we have

$$\begin{cases} u_N(\mathbf{x};\mathbf{s},\mathbf{c}) = \sum\limits_{i=1}^{N} c_i Ln\left(|\mathbf{x}-\mathbf{s}_i|\right) \\ \text{for Laplacian;} \\ u_N(\mathbf{x};\mathbf{s},\mathbf{c}) = \sum\limits_{i=1}^{N} c_i H^{(1)}\left(|\mathbf{x}-\mathbf{s}_i|\right) \\ \text{for Helmholtz operator;} \\ u_N(\mathbf{x};\mathbf{s},\mathbf{c}) = \sum\limits_{i=1}^{N} c_i K_0\left(|\mathbf{x}-\mathbf{s}_i|\right) \\ \text{for modified Helmholtz operator;} \\ u_N(\mathbf{x};\mathbf{s},\mathbf{c}) = \begin{cases} \sum\limits_{i=1}^{N} c_{1i} Ln\left(|\mathbf{x}-\mathbf{s}_i|\right) \\ + \sum\limits_{i=1}^{N} c_{2i} |\mathbf{x}-\mathbf{s}_i|^2 Ln\left(|\mathbf{x}-\mathbf{s}_i|\right) \end{cases} \\ \text{for biharmonic operator.} \end{cases} \tag{4}$$

where, $H_0^{(1)}(kr)$ is the Hankel function of the first kind of order zero, and K_0 is the modified Bessel function of the second kind of order zero. In the MFS, the source intensities $\mathbf{c}$ are determined so that the boundary condition is satisfied at N boundary points, $(\mathbf{x}_1, \mathbf{x}_2, ..., \mathbf{x}_N)$. This yields a linear system of the following form, and can then be solved.

$$\mathbf{Gc} = \mathbf{f} \tag{5}$$

where $\mathbf{f}$ is composed by the boundary conditions and $\mathbf{G}$ is the system matrix such that $\mathbf{G}_{ij} = G(\mathbf{x}_i;\mathbf{s}_j)$.

3 Condition number and error

In order to analyze the accuracy of the MFS, we define the condition number as following:

$$\text{CDN} = \frac{\text{maximum singular value}}{\text{minimum singular value}} \tag{6}$$

There are several algorithms provide estimates of CDN that do not actually obtain the exact singular values. In this paper we utilize the LINPACK's Cholesky decomposition [Anderson, Bai, Bischof, Blackford, Demmel, Dongarra, Croz, Greenbaum, Hammarling, McKenney and Sorensen (1979)] to obtain the CDN. However, it

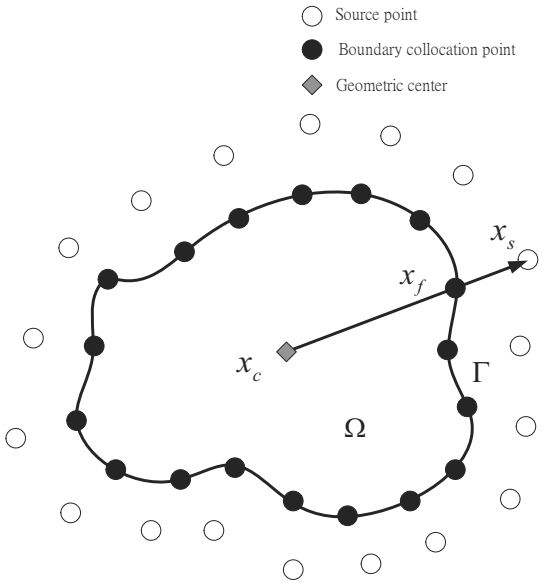

Figure 1 : Schematic diagram of the source and boundary field points.

should be noticed that the accuracy of CDN itself is dependent on the precision which will be discussed in the section of results and discussions.

On the other hand, we define the following root-mean-square error for our analysis:

$$\text{r.m.s} = \sqrt{\frac{\sum_{i=1}^{M} (u_{numerical,i} - u_{exact,i})^2}{M}} \tag{7}$$

in which M is the total number of points considered, $u_{exact,i}$ is the exact solution at point i, and $u_{numerical,i}$ is the numerical solution at the point i.

4 Boundary collocation points and source points

The distributions of the source points and boundary collocation points are significant in the MFS. Bogomolny (1985) located the sources uniformly in a circle enclosing the computational domain. On the other, Heise (1976) chose the sources by stipulating auxiliary source curve to be equidistant from boundary. In our experiences, Heise's method generally gives better results for computational domain of slender shapes. Accordingly, we suggest the following procedure to locate the sources.

Consider a radial convex computational domain as depicted in Fig 1, where Ω is the computational domain and Γ is the boundary of Ω. Here, a radial convex shape is defined by crossing boundary exactly twice for any line passing the geometric center of the shape. Then, we introduce a procedure to locate source points and boundary collocation points for radial convex shapes:

Part I (Locations of boundary collocation & source points)

Step 1: The boundary collocation points are uniformly distributed on the boundary Γ

Step 2: According to the boundaries of the physical domain, the geometric center,$\mathbf{x}_c$, is then obtained.

Step 3: The distributions of the source points are arranged by the following equation:

$$\mathbf{x}_s = \mathbf{x}_f + \lambda(\mathbf{x}_f - \mathbf{x}_c) \tag{8}$$

where $\mathbf{x}_s$ and $\mathbf{x}_f$ are the spatial coordinates of the source and boundary points, respectively. Also, λ is defined as the parameter of source location. Therefore, the distributions of the source points can be obtained once the parameter of source location,λ, is determined. The geometrical configuration of the procedure is described in Fig. 1. For problems without exact solutions, the following procedure is suggested to locate the sources:

Part II (Determination of λ)

Step 1: Set up some exact solutions and carry out several numerical experiments to sketch figures of CDN v.s. λ and r.m.s v.s. λ. Then, determine the limit of equation solver from the figures. Details about the determination are stated in the section of numerical results.

Step 2: Solve the desired problem by the MFS and draw the figure of CDN v.s. λ.

Step 3: Select λ for which CDN near the limit of equation solver from the figure in the last step. And, solve the problem by the selected λ.

In our numerical experiments, four shapes are considered: a circle, a square, a rectangle, and a peanut (Fig. 2 & Fig. 3). Generally, it is not easy to define a procedure to locate the source points for arbitrary shapes, such as concave shapes or degenerate boundaries. In this kind of situations, nonlinear optimization [Mathon and Johnston (1977)] or domain decomposition method [Young, Fan, Tsai and Chen (2006)] is suggested. Nevertheless, it is convinced that the proposed procedure is sufficient

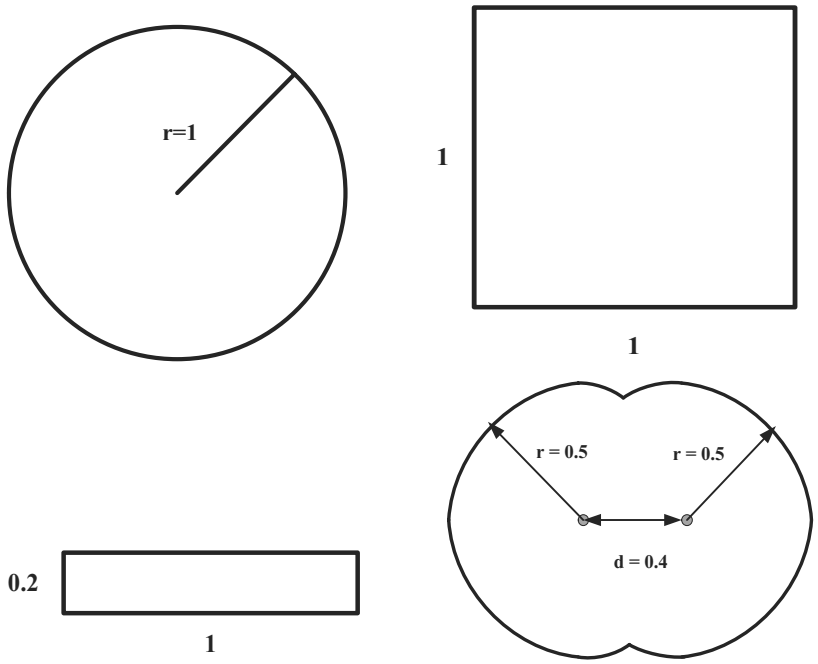

Figure 2 : Schematic diagrams of different shapes of computational domains.

for most of the computational domains according to our numerical results.

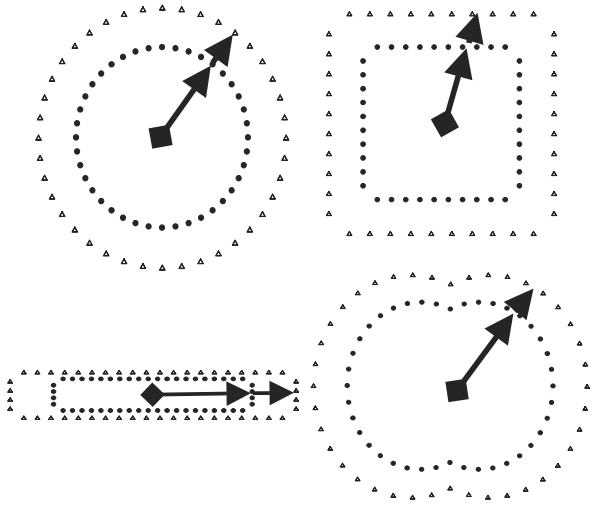

Figure 3 : Schematic diagrams of the distribution of source and boundary field points. ($x_f : \bullet; x_c : \diamond; x_s : \triangle$)

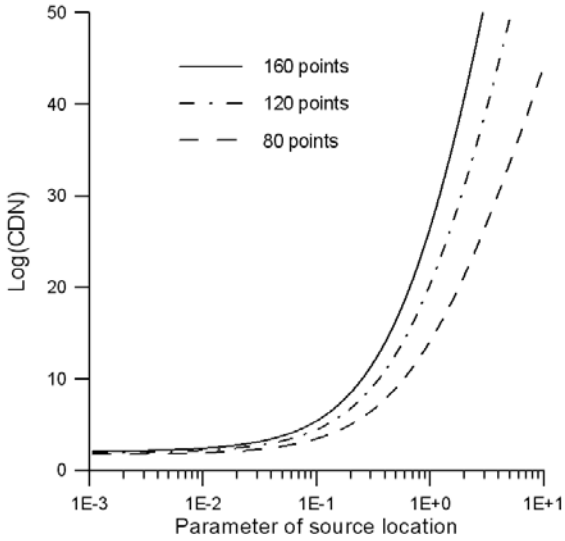

Figure 4 : Analytical values of Log(CDN) v.s. parameter of source location $(R/a-1)$ for a circle with radius $a=1$.

5 Theoretical statements

The proposed procedure of locating sources is developed based on general relations among the error, source locations, and condition number. Theoretically, it is proved that worse conditioning [Lyngby (1981)] and better accuracy [Mathon and Johnston (1977), Bogomolny (1985)] are resulted when the sources are located farther in a proper way.

Consider a Laplace problem defined in equation (1) with

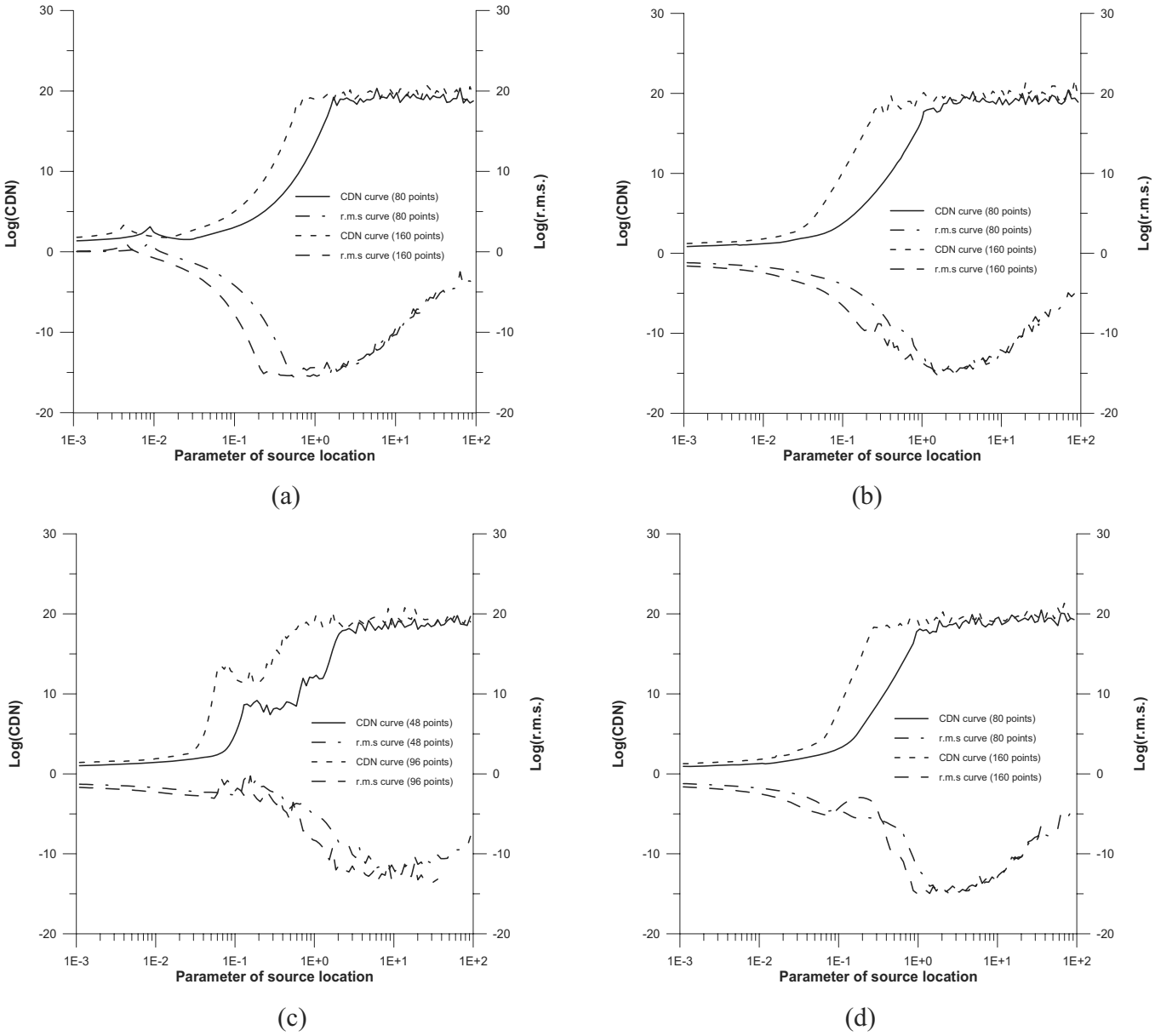

Figure 5 : Comparison of the shapes of computational domains in Laplace equation with Dirichlet boundary condition, for (a) circle (b) square (c) rectangle (d) peanut.

$L = \nabla^2$ and $\Omega = \{\mathbf{x} = (x,y) | x^2 + y^2 \leq a^2\}$. Bogomolny (1985) proved the following error estimate:

$$\underset{\mathbf{x}\in\Gamma}{MAX} |u(\mathbf{x}) - u_N(\mathbf{x})| \leq \frac{K(\varepsilon, R)}{n^{q+\gamma-\varepsilon}} \tag{9}$$

where $u_N(\mathbf{x})$ is the MFS approximation defined by equation (2), $\varepsilon > 0$ is a prescribed parameter, $R = (1+\lambda)a$ is the radius of the source points, n is the number of harmonic modes considered, and q & γ are the exponents of smoothness for f and Γ respectively. In the estimate, $K(\varepsilon, R)$ is proved to be a monotonically decreasing function of R. Details can be found in the reference [Bogomolny (1985)].

On the other hand, Lyngby (1981) derived the following

formula for the CDN of the resulted system matrix:

$$CDN = \begin{cases} \frac{1}{2(\frac{R}{a})|LogR|} \text{ for } \begin{cases} e^{\frac{-1}{N(\frac{R}{a})^{\frac{N}{2}}}} \le R < 1 \\ 1 < R \le e^{\frac{1}{N(\frac{R}{a})^{\frac{N}{2}}}} \end{cases} \\ \frac{N}{2}(\frac{R}{a})^{\frac{N}{2}-1} \text{ for } \begin{cases} e^{\frac{-a}{2R}} \le R < e^{\frac{-1}{N(\frac{R}{a})^{\frac{N}{2}}}} \\ e^{\frac{1}{N(\frac{R}{a})^{\frac{N}{2}}}} < R \le e^{\frac{a}{2R}} \end{cases} \\ N|LogR|(\frac{R}{a})^{\frac{N}{2}} \text{ for } \begin{cases} 0 \le R < e^{\frac{-a}{2R}} \\ e^{\frac{a}{2R}} < R \end{cases} \end{cases} \quad (10)$$

Figure 4 depicts the plots of Log(CDN) v.s. parameter of source location $(R/a-1)$ for $a=1$, in which it is found CDN is a monotonically increasing function of R. Moreover, the cases of finer nodes give higher CDN if same parameter of source location is utilized.

In order to obtain the best accuracy, our basic idea is to increase R as large as possible once the CDN does not exceed the limit of equation solver. For computational domains other than a circle, our numerical results also demonstrate similar behaviors among the error, CDN, and parameter of source location.

6 Numerical results and Discussions

In order to check the relations among the error, source locations, and condition number, the following five cases are tested: Laplace equation with Dirichlet boundary condition, Helmholtz equation with Dirichlet boundary condition, Helmholtz equation with Neumann boundary condition, modified Helmholtz equation with Dirichlet boundary condition, and biharmonic equation with essential boundary conditions. On the other hand, four shapes are considered in all these five cases: a circle, a square, a rectangle, and a peanut (Fig. 2).

Laplace equation with Dirichlet boundary condition

The following Laplace problems are solved by the MFS:

$$\begin{aligned} &G.E.: \nabla^2 u = 0 \text{ in } \Omega \\ &B.C.: u(x,y) = \begin{cases} \cos(x)\cosh(y) \\ +\sin(x)\sinh(y) \end{cases} \text{ on } \Gamma \end{aligned} \quad (11)$$

The exact solution of the problem is

$$u(x,y) = \cos(x)\cosh(y) + \sin(x)\sinh(y) \quad (12)$$

The results of the condition number tests are demonstrated in Fig. 5. There are four curves in all figures. The upper two curves are the CDN v.s. parameter of source location for coarse and fine source points. In all the figures, accurate CDNs are obtained up to $10^{17} \sim 10^{18}$ in which the LINPACK's Cholesky decomposition [Anderson, Bai, Bischof, Blackford, Demmel, Dongarra, Croz, Greenbaum, Hammarling, McKenney and Sorensen (1979)] and double precision (8 BYTE) are adopted. The other two curves are the r.m.s v.s. parameter of source location for coarse and fine source points. From Fig. 5, it is easy to conclude that r.m.s reaches it best value $10^{-11} \sim 10^{-14}$ once CDN approaches the limit of equation solver $10^{17} \sim 10^{18}$. On the other hand, the cases of finer nodes generally give higher CDN, and better accuracy is achieved if same parameter of source location is utilized. Moreover, the numerical CDN of the circle problem shows good agreements with the analytical values depicted in Fig. 4.

Helmholtz equation with Dirichlet boundary condition

On the other hand, the following Dirichlet Helmholtz problems in a circle, a square, a rectangle, and a peanut respectively, depicted in Fig. 2, are adopted:

$$\begin{aligned} &\nabla^2 u + \left[\left(\frac{\pi}{2.1}\right)^2 + \left(\frac{\pi}{2.3}\right)^2\right] u = 0 \text{ in } \Omega \\ &u(x,y) = \sin\left(\frac{\pi x}{2.1}\right)\sin\left(\frac{\pi y}{2.3}\right) \text{ on } \Gamma \end{aligned} \quad (13)$$

$$\begin{aligned} &\nabla^2 u + \left[\left(\frac{\pi}{1.1}\right)^2 + \left(\frac{\pi}{1.3}\right)^2\right] u = 0 \text{ in } \Omega \\ &u(x,y) = \sin\left(\frac{\pi x}{1.1}\right)\sin\left(\frac{\pi y}{1.3}\right) \text{ on } \Gamma \end{aligned} \quad (14)$$

$$\begin{aligned} &\nabla^2 u + \left[\left(\frac{\pi}{1.1}\right)^2 + \left(\frac{\pi}{1.1}\right)^2\right] u = 0 \text{ in } \Omega \\ &u(x,y) = \sin\left(\frac{\pi x}{1.1}\right)\sin\left(\frac{\pi y}{1.1}\right) \text{ on } \Gamma \end{aligned} \quad (15)$$

$$\begin{aligned} &\nabla^2 u + \left[\left(\frac{\pi}{2.1}\right)^2 + \left(\frac{\pi}{2.3}\right)^2\right] u = 0 \text{ in } \Omega \\ &u(x,y) = \sin\left(\frac{\pi x}{2.1}\right)\sin\left(\frac{\pi y}{2.3}\right) \text{ on } \Gamma \end{aligned} \quad (16)$$

in which their exact solutions are

$$u(x,y) = \sin\left(\frac{\pi x}{2.1}\right)\sin\left(\frac{\pi y}{2.3}\right) \quad (17)$$

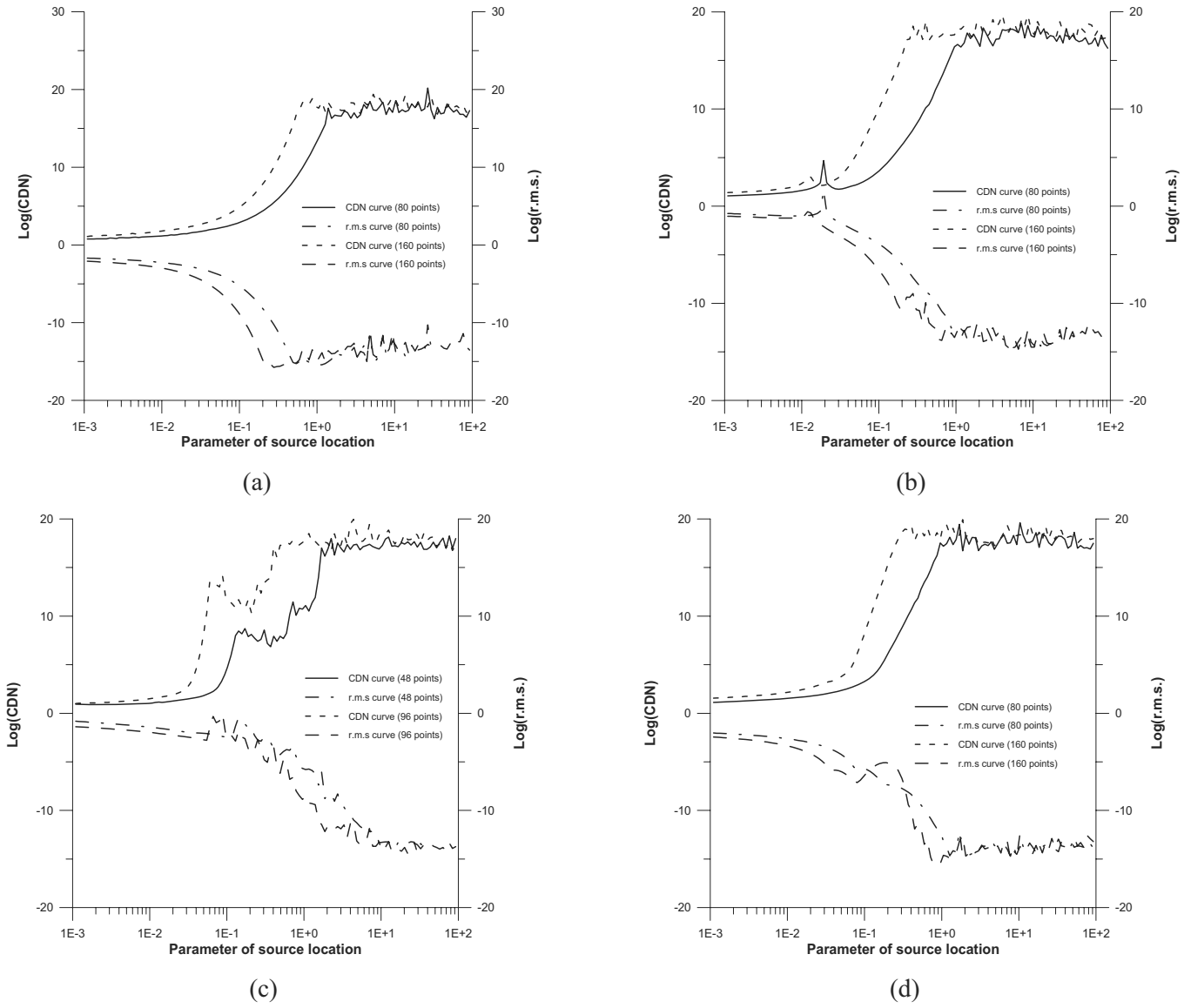

Figure 6 : Comparison of the shapes of computational domains in Helmholtz equation with Dirichlet boundary condition, for (a) circle (b) square (c) rectangle (d) peanut.

$$u(x,y) = \sin\left(\frac{\pi x}{1.1}\right)\sin\left(\frac{\pi y}{1.3}\right) \tag{18}$$

$$u(x,y) = \sin\left(\frac{\pi x}{1.1}\right)\sin\left(\frac{\pi y}{1.1}\right) \tag{19}$$

$$u(x,y) = \sin\left(\frac{\pi x}{2.1}\right)\sin\left(\frac{\pi y}{2.3}\right) \tag{20}$$

The results of the condition number tests are described in Fig. 6. It is also observed that r.m.s reaches it best value $10^{-11} \sim 10^{-14}$ once CDN approaches the limit of equation solver $10^{17} \sim 10^{18}$.

Helmholtz equation with Neumann boundary condition

Similarly, the following Neumann Helmholtz problems in a circle, a square, a rectangle, and a peanut respectively, depicted in Fig. 2, are solved by the MFS:

$$\begin{aligned} &\nabla^2 u + \left[\left(\frac{\pi}{2.1}\right)^2 + \left(\frac{\pi}{2.3}\right)^2\right] u = 0 \; in \; \Omega \\ &\frac{\partial u(x,y)}{\partial n} = \mathbf{n}\cdot\nabla\left(\sin\left(\frac{\pi x}{2.1}\right)\sin\left(\frac{\pi y}{2.3}\right)\right) \text{ on } \Gamma \end{aligned} \tag{21}$$

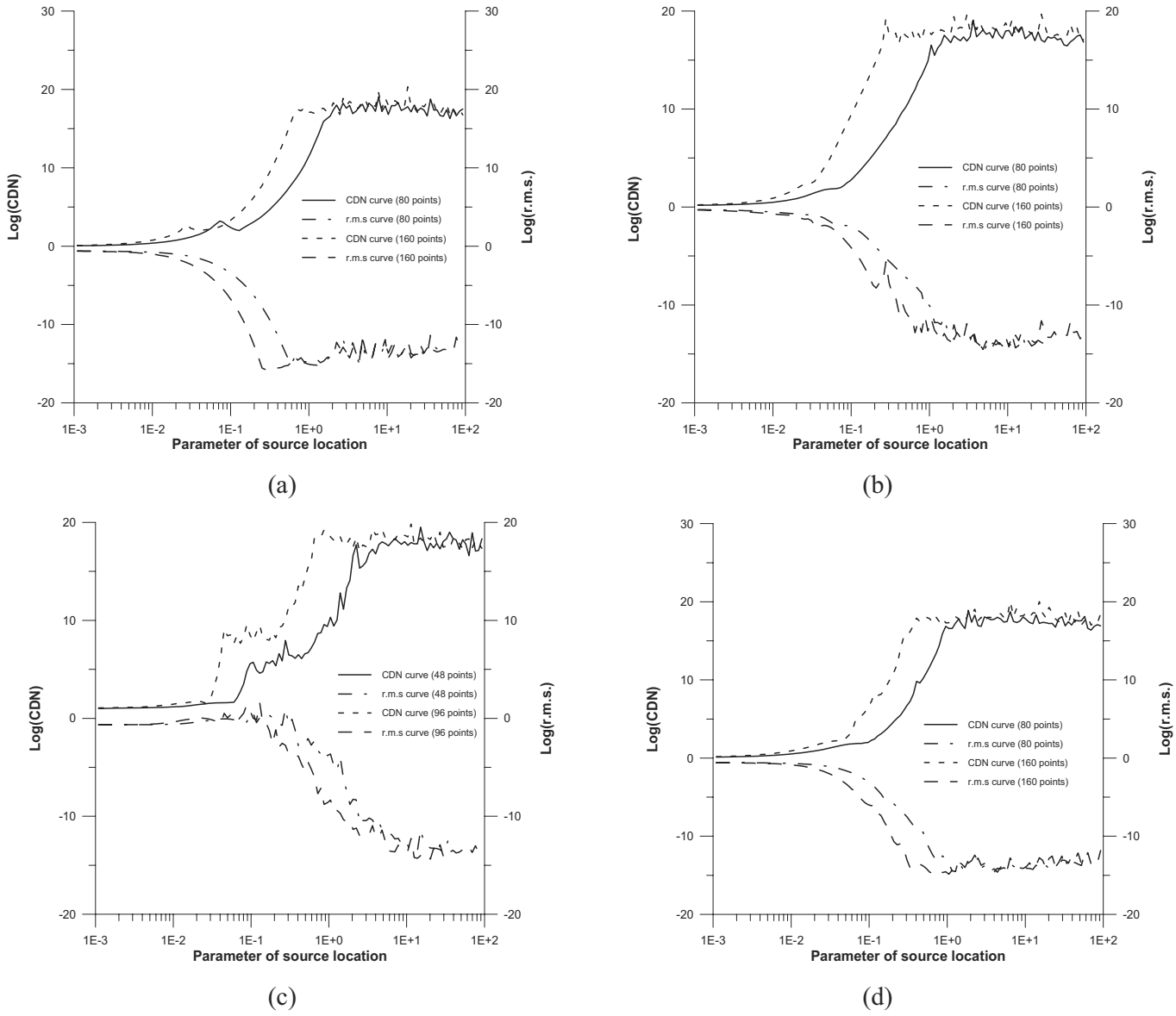

Figure 7 : Comparison of the shapes of computational domains in Helmholtz equation with Neumann boundary condition, for (a) circle (b) square (c) rectangle (d) peanut.

$$\nabla^2 u + \left[\left(\frac{\pi}{1.1}\right)^2 + \left(\frac{\pi}{1.3}\right)^2\right] u = 0 \; in \; \Omega$$
$$\frac{\partial u(x,y)}{\partial n} = \mathbf{n} \cdot \nabla(\sin\left(\frac{\pi x}{1.1}\right) \sin\left(\frac{\pi y}{1.3}\right)) \text{ on } \Gamma \qquad (22)$$

$$\nabla^2 u + \left[\left(\frac{\pi}{1.1}\right)^2 + \left(\frac{\pi}{1.1}\right)^2\right] u = 0 \; in \; \Omega$$
$$\frac{\partial u(x,y)}{\partial n} = \mathbf{n} \cdot \nabla(\sin\left(\frac{\pi x}{1.1}\right) \sin\left(\frac{\pi y}{1.1}\right)) \text{ on } \Gamma \qquad (23)$$

$$\nabla^2 u + \left[\left(\frac{\pi}{2.1}\right)^2 + \left(\frac{\pi}{2.3}\right)^2\right] u = 0 \; in \; \Omega$$
$$\frac{\partial u(x,y)}{\partial n} = \mathbf{n} \cdot \nabla(\sin\left(\frac{\pi x}{2.1}\right) \sin\left(\frac{\pi y}{2.3}\right)) \text{ on } \Gamma \qquad (24)$$

with the following exact solutions:

$$u(x,y) = \sin\left(\frac{\pi x}{2.1}\right) \sin\left(\frac{\pi y}{2.3}\right) \qquad (25)$$

$$u(x,y) = \sin\left(\frac{\pi x}{1.1}\right) \sin\left(\frac{\pi y}{1.3}\right) \qquad (26)$$

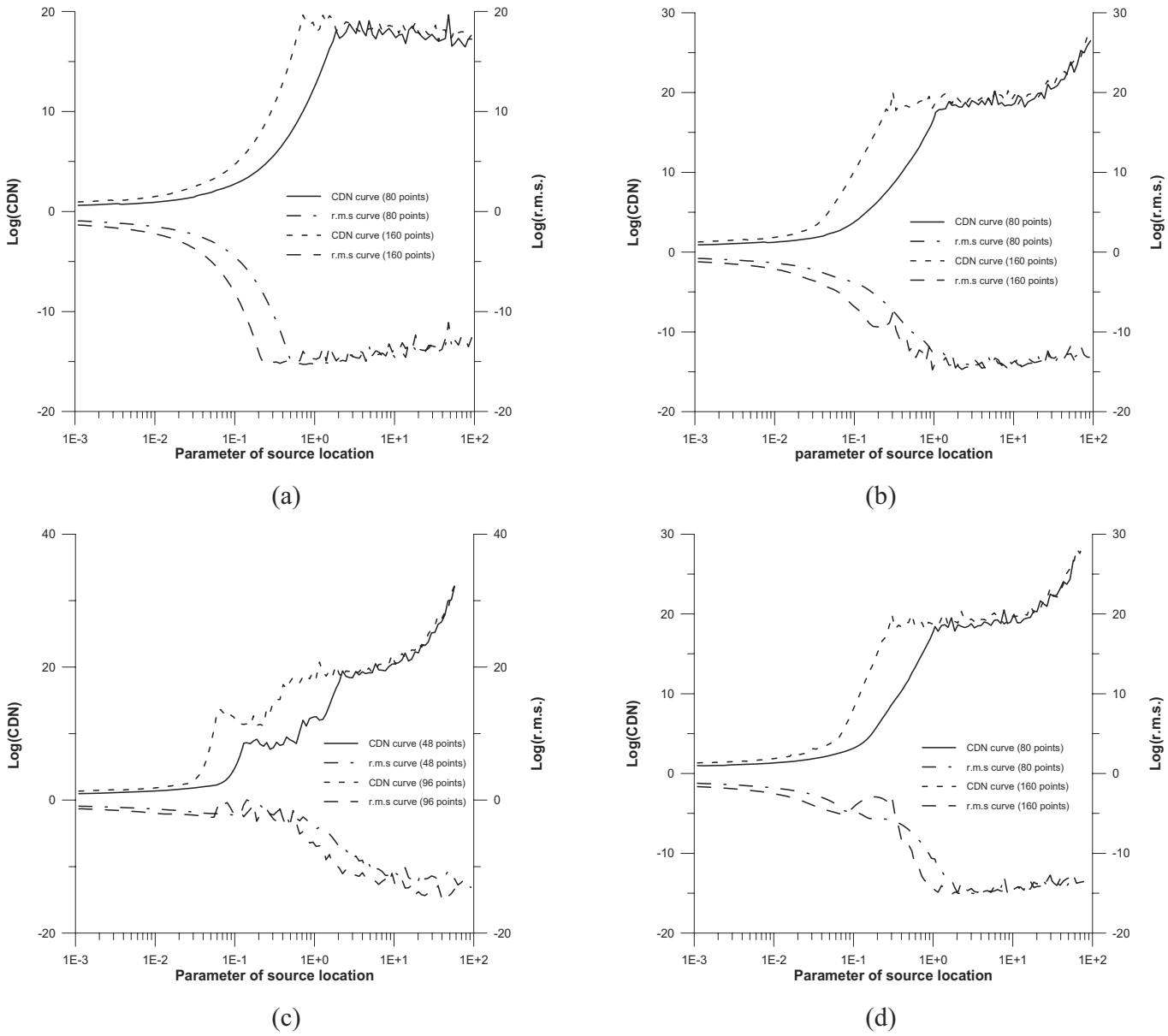

Figure 8 : Comparison of the shapes of computational domains in Helmholtz equation with Neumann boundary condition, for (a) circle (b) square (c) rectangle (d) peanut.

$$u(x,y) = \sin\left(\frac{\pi x}{1.1}\right)\sin\left(\frac{\pi y}{1.1}\right) \tag{27}$$

$$u(x,y) = \sin\left(\frac{\pi x}{2.1}\right)\sin\left(\frac{\pi y}{2.3}\right) \tag{28}$$

Also, the condition number tests are depicted in Fig. 7. It is also observed that r.m.s reaches it best value $10^{-11} \sim 10^{-14}$ once CDN approaches the limit of equation solver $10^{17} \sim 10^{18}$.

Modified Helmholtz equation with Dirichlet boundary condition

The numerical experiments can be extended to modified Helmholtz equation with Dirichlet boundary condition easily. The following problem is considered.

$$\begin{aligned} &\nabla^2 u - \left(1^2 + 1^2\right) u = 0 \text{ i}n\ \Omega \\ &u(x,y) = \exp^{(x+y)} \text{ on } \Gamma \end{aligned} \tag{29}$$

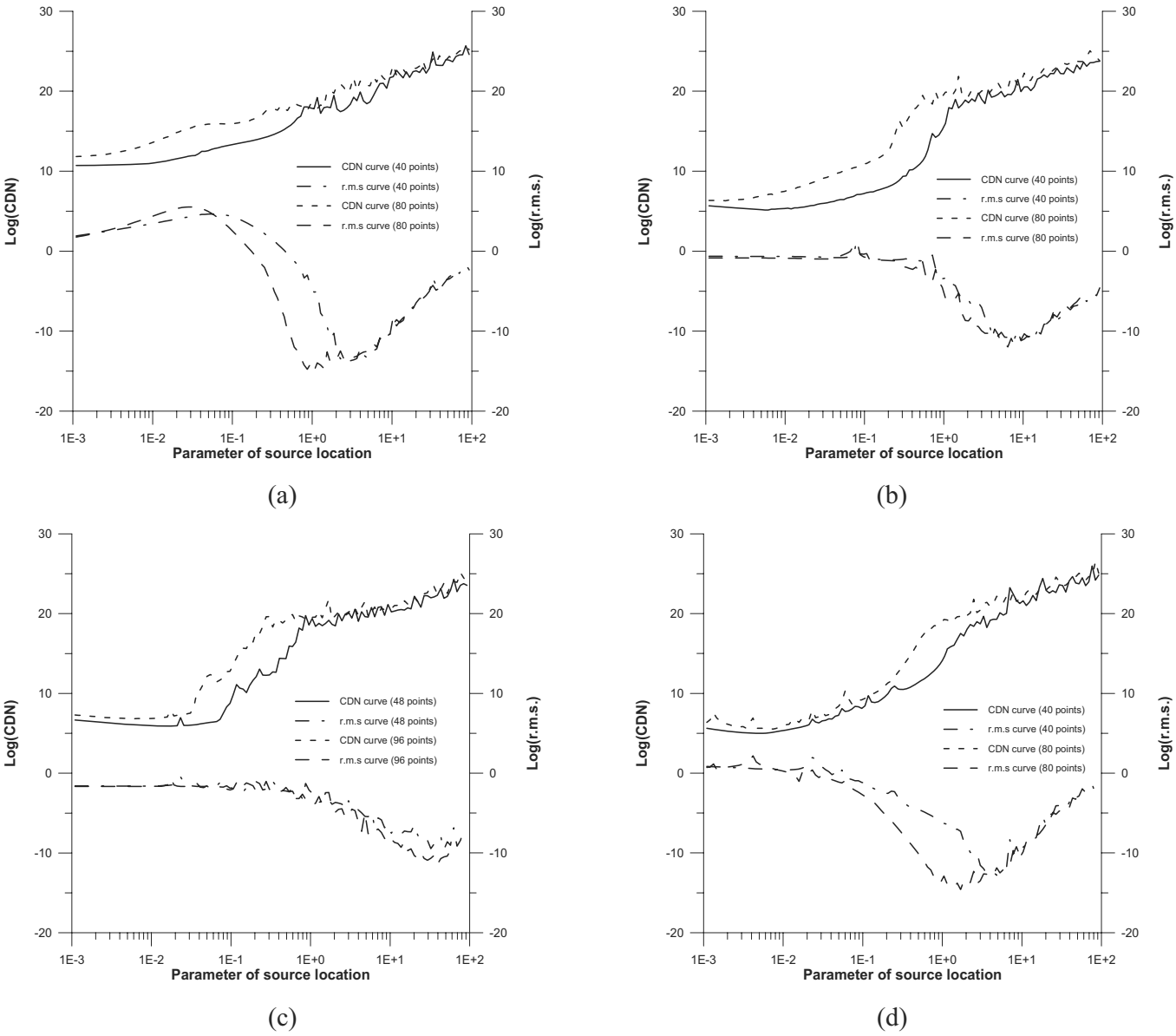

Figure 9 : Comparison of the shapes of computational domains in biharmonic equation with essential boundary condition, for (a) circle (b) square (c) rectangle (d) peanut.

with exact solution

$$u(x,y) = \exp^{(x+y)} \tag{30}$$

The condition number tests in the four shapes are depicted in Fig. 8. In which the r.m.s also reaches it best value $10^{-11} \sim 10^{-14}$ once CDN approaches the limit of equation solver $10^{17} \sim 10^{18}$.

Biharmonic equation with essential boundary conditions

Numerical experiments are also carried out for biharmonic equation with essential boundary conditions. The numerical results are generally same although the governing equation is fourth order.

$$\begin{aligned} &\nabla^4 u = 0 \; in \; \Omega \\ &u(x,y) = \begin{cases} \cos(x)\cosh(y) \\ +\sin(x)\sinh(y) \end{cases} \quad \text{on } \Gamma \\ &\frac{\partial u(x,y)}{\partial n} = \begin{cases} \mathbf{n}\cdot\nabla(\cos(x)\cosh(y) \\ +\sin(x)\sinh(y)) \end{cases} \quad \text{on } \Gamma \end{aligned} \tag{31}$$

with exact solution

$$u(x,y) = \cos(x)\cosh(y) + \sin(x)\sinh(y) \tag{32}$$

Similar results of condition number tests are also obtained as sketched in Fig. 9. However, the CDN is generally higher since the governing equation is fourth order and bigger system matrix should be solved.

7 Conclusions

A procedure is suggested to locate the sources points of computational domains of radial convex shapes. The following numerical experiments are carried out: Laplace equation with Dirichlet boundary condition, Helmholtz equation with Dirichlet boundary condition, Helmholtz equation with Neumann boundary condition, modified Helmholtz equation with Dirichlet boundary condition, and biharmonic equation with essential boundary conditions. Moreover, four typical shapes are considered in these five cases: a circle, a square, a rectangle, and a peanut. The LINPACK's Cholesky decomposition [Anderson, Bai, Bischof, Blackford, Demmel, Dongarra, Croz, Greenbaum, Hammarling, McKenney and Sorensen (1979)] and double precision (8 BYTE) are adopted in these numerical experiments. In the numerical experiments, higher condition numbers and smaller errors are observed when the sources are located farther in a proper way. And, the r.m.s of numerical results generally reach their best values $10^{-11} \sim 10^{-14}$ once CDN approaches the limit of equation solver $10^{17} \sim 10^{18}$. Moreover, the cases of finer nodes give higher CDN, and better accuracy is achieved if same parameter of source location is utilized in the same case.

Therefore, it is convinced that the proposed procedure of locating sources can be practically applied to time-independent partial differential equations without exact solutions and general high accurate solutions are obtained. Of course, it is not easy to define a general procedure to locate the source points for arbitrary shapes. We suggest the nonlinear optimization [Mathon and Johnston (1977)] or domain decomposition method [Young, Fan, Tsai and Chen (2006)] for problems with these complex computation domains. Nevertheless, the procedure is practically useful for most of the computational domains.

Acknowledgement: The National Science Council of Taiwan is gratefully acknowledged for providing financial support to carry out the present work under the Grant No. NSC 93-2611-E-002-001, NSC95-2221-E-002-406 NSC and 95-2221-E-464-002. The third author acknowledges the support from Center for Aerospace Research and Education, University of California, Irvine, while he was a visiting scholar.

References

Atluri, S.N. (2004): The meshless method (MLPG) for domain & BIE discretization. 700 pages, *Tech Science Press*, Forsyth, GA,USA.

Anderson, E.; Bai, Z.; Bischof, C.; Blackford, L.S.; Demmel, J.; Dongarra, J.; Croz, J.D.; Greenbaum, A.; Hammarling, S.; McKenney, A.; Sorensen, D. (1979): Linpack user's guide, *SIAM*, Philadelphia,PA,USA.

Bogomolny, A. (1985): Fundamental solutions method for elliptic boundary value problems, *SIAM Journal of Numerical Analysis*, vol. 22, pp. 644-669.

Chen C.W.; Fan, C.M.; Young, D.L.; Murugesan, K.T; Tsai, C.C (2005): Eigenanalysis for membranes with stringers using the methods of fundamental solutions and domain decomposition. *CMES: Computer Modeling in Engineering & Sciences*, vol. 8(1), pp. 29-44.

Han, Z.D.; Atluri, S.N. (2004): A meshless local Petrov-Galerkin (MLPG) approach for 3-dimensional elasto-dynamics. *CMC: Computers, Materials & Continua,* vol. 1(2), pp. 129-140.

Heise, U. (1976): Numerical properties of integral equations in which the given boundary values and the sought solutions are defined on different curves, *Computers & Structures*, vol. 8, pp. 199-205.

Hon, Y.C.; Wei, T. (2005): The method of fundamental solution for solving multidimensional inverse heat conduction problems. *CMES: Computer Modeling in Engineering & Sciences*, vol. 7(2), pp. 119-132.

Kansa, E.J. (1990A): Multiquadrics - a scattered data approximation scheme with applications to computational fluid dynamics-I. Surface approximations and partial derivative estimates. *Computers and Mathematics with Applications*, vol. 19, pp. 127-145.

Kansa, E.J. (1990B): Multiquadrics - a scattered data approximation scheme with applications to computa-

tional fluid dynamics-II. Solutions to parabolic, hyperbolic and elliptic partial differential equations. *Computers and Mathematics with Applications*, vol. 19, pp. 147-161.

Kim, H.G.; Atluri, S.N. (2000): Arbitrary placement of secondary nodes, and error control, in the meshless local Petrov-Galerkin (MLPG) method. *CMES: Computer Modeling in Engineering & Sciences*, vol. 1(3), pp. 11-32.

Kupradze, V.D.; Aleksidze, M.A. (1964): The method of functional equations for the approximate solution of certain boundary value problems, *USSR Computational Mathematics and Mathematical Physics*, vol. 4, pp. 82-126.

Li, J.; Cheng, A.H.-D.; Chen, C.S. (2003): A comparison of efficiency and error convergence of multiquadric collocation method and finite element method. *Engineering Analysis with Boundary Elements,* vol. 27, pp. 251-257.

Lin, H.; Atluri S.N. (2000): Meshless local Petrov-Galerkin (MLPG) method for convection-diffusion problems. *CMES: Computer Modeling in Engineering & Sciences*, vol. 1(2), pp. 45-60.

Lyngby, S.C. (1981): Condition number of matrices derived from two classes of integral equations. *Mathematical Methods in the Applied Sciences*, vol. 3, pp. 364-392.

Mathon, R.; Johnston, R.L. (1977): The approximate solution of elliptic boundary-value problems by fundamental solutions. *SIAM Journal on Numerical Analysis*, vol. 14, pp. 638-650.

Smyrlis, Y.S.; Karageorghis, A. (2001): Some aspects of the method of fundamental solutions for certain harmonic problems. *Journal of Scientific Computing*, vol. 16, pp. 341-371.

Smyrlis, Y.S.; Karageorghis, A. (2004): A linear least-square MFS for certain elliptic problems. *Numerical Algorithms* vol. 35, pp. 29-44.

Tsai, C.C.; Young, D.L.; and Cheng, A.H.-D. (2002): Meshless BEM for three-dimensional Stokes flows, *CMES: Computer Modeling in Engineering & Sciences*, vol. 3, pp. 117-128.

Wordelman, C.J.; Aluru, N.R.; Ravaioli, U. (2000): A meshless method for the numerical solution of the 2- and 3-D Semiconductor Poisson equation. *CMES: Computer Modeling in Engineering & Sciences*, vol. 1(1), pp. 121-126.

Young, D.L.; Chen, C.S.; Wong, T.K. (2005): Solution of Maxwell's equations using the MQ method. *CMC: Computers, Materials & Continua,* Vol. 2(4), pp. 267-276.

Young, D.L.; Jane, S.C.; Lin, C.Y.; Chiu, C.L.; Chen, K.C. (2004): Solutions of 2D and 3D Stokes laws using multiquadrics method. *Engineering Analysis with Boundary Elements*, vol. 28, pp. 1233-1243.

Young, D.L.; Fan, C.M.; Tsai, C.C.; Chen, C.W. (2006): The method of fundamental solutions and domain decomposition method for degenerate seepage flownet problems. *Journal of the Chinese Institute of Engineers*, vol. 29(1), pp. 63-73.

Young, D.L.; Tsai, C.C.; Lin, Y.C.; Chen, C.S. (2006): The method of fundamental solutions for eigenfrequencies of plate vibrations. *CMC: Computers, Materials & Continua,* Vol. 4, No. 1, pp. 1-10.

Young, D.L.; Ruan J.W. (2005): Method of fundamental solutions for scattering problems of electromagnetic waves. *CMES: Computer Modeling in Engineering & Sciences*, Vol. 7(2), pp. 223-232.